# Stable Silicon Isotopic Compositions of the Lena River and its Tributaries: Implications for Silicon Delivery to the Arctic Ocean

Xiaole Sun[1,2*], Carl-Magnus Mörth[3], Don Porcelli[4], Liselott Kutscher[3,5], Catherine Hirst[3,5], Melissa J. Murphy[4], Trofim Maximov[6,7], Roman E. Petrov[6,7], Christoph Humborg[1,2], Melanie Schmitt[5], Per S. Andersson[5]

[1] Baltic Sea Center, Stockholm University, SE-106 91, Stockholm, Sweden

[2] Department of Environmental Science and Analytical Chemistry, Stockholm University, SE- 106 91, Stockholm, Sweden

[3] Department of Geological Sciences, Stockholm University, SE-106 91, Stockholm, Sweden

[4] Department of Earth Sciences, Oxford University, OX1 3AN, Oxford, UK

[5] Department of Geosciences, Swedish Museum of Natural History, SE-104 05, Stockholm, Sweden

[6] Institute of Biological Problems of the Cryolithozone, Yakutsk, 677891, Russia

[7] Institute for Natural Sciences of North-Eastern Federal University, Yakusk, Russia

[*]Correspondence to Xiaole Sun, Email: xiaole.sun@su.se

**Abstract**

Silicon isotope values ($\delta^{30}Si_{DSi}$) of dissolved silicon (DSi) have been analyzed in the Lena River and its tributaries, one of the largest Arctic watersheds in the world. The geographical and temporal variations of $\delta^{30}Si_{DSi}$ range from +0.39 to +1.86‰ with DSi concentrations from 34 to 121 μM. No obvious patterns of DSi concentrations and $\delta^{30}Si_{DSi}$ values were observed along over 200 km of the two major tributaries, the Viliui and Aldan Rivers. In summer, the variations of DSi concentrations and $\delta^{30}Si_{DSi}$ values in the water are either caused by biological uptake by higher plants and phytoplankton or by mixing of water masses carrying different DSi concentrations and $\delta^{30}Si_{DSi}$ values. DSi in tributaries from the Verkhoyansk Mountain Range seems to be associated with secondary clay formation that increased the $\delta^{30}Si_{DSi}$ values, while terrestrial biological production is likely more prevalent in controlling $\delta^{30}Si_{DSi}$ values in Central Siberian Plateau and Lena Amganski Inter-River Area. In winter, when soils were frozen, the $\delta^{30}Si_{DSi}$ values in the river appeared to be controlled by weathering and clay formation in deep intrapermafrost groundwater. During the spring flood, dissolved silicate materials and phytoliths were flushed from the upper thawed soils into rivers, which reset $\delta^{30}Si_{DSi}$ values to the values observed prior to the biological bloom in summer. The results indicate that the Si isotope values reflect the changing processes controlling Si outputs to the Lena River and to the Arctic Ocean between seasons. The annual average $\delta^{30}Si_{DSi}$ value of the Lena Si flux is calculated to be +0.86±0.3‰ using measured $\delta^{30}Si_{DSi}$ values from each season. Combined with the estimate of +1.6±0.25‰ for the Yenisey River, an updated $\delta^{30}Si_{DSi}$ value of the major river Si inputs to the Arctic Ocean is estimated to be +1.3±0.3‰. This value is expected to shift towards higher values in the future because of the impacts from a variety of biological and geochemical processes and sources under global warming.

**Key words**: silicon isotopes, Lena River, tributary, Arctic, seasonality

## 1. Introduction

Silicate weathering on the continents controls the delivery of dissolved silicon (as $H_4SiO_4$, referred to as DSi) and other elements to the ocean, which in turn plays an important role in regulating ocean primary production and $CO_2$ exchange between the atmosphere and the ocean (e.g. Tréguer and De La Rocha, 2013). However, not all DSi released by weathering is transported via rivers and ultimately reaches the ocean. DSi from silicate weathering is also released to soil water and groundwater, incorporated into secondary minerals or taken up by terrestrial plants in the form of amorphous silica, while the remaining part of DSi is delivered to rivers. The fate of DSi during river transport is dependent upon uptake into siliceous phytoplankton and periphyton (e.g. diatoms), which therefore impact the DSi prior to discharge to the ocean (e.g. Cornelis et al., 2011). Understanding these processes still remains challenging, especially in the pan-arctic region, where there are strong seasonal variations of temperature and water discharge, and rapid changes due to global warming.

The world's ocean receives 371 000 Gg/yr of DSi from continental runoff (Dürr et al., 2011), of which roughly 11 395 Gg Si/yr are delivered from pan-arctic areas to the Arctic Ocean (Holmes et al., 2011). Normalized to the ocean volume, this is three and seven times the riverine DSi flux delivered to the Atlantic and Pacific Ocean, respectively, and approximately five times the average global flux to the oceans (Dürr et al., 2011). In the Arctic regions, a warmer climate has led to changes in precipitation regimes, increased thickness of the active layer of permafrost soils and permafrost degradation (Frey and McClelland, 2009). These changes have the potential to decrease riverine DSi concentrations and reduce DSi delivery to the Arctic Ocean, which has been predicted by the " substituting space-for-time" approach

(Pokrovsky et al. 2015; Vorobyev et al. 2017). However, the mechanisms controlling the fate of Si remain poorly understood, especially with regard to the seasonal variations of the Si river flux.

Stable Si isotopes in surface environments have been shown to be useful to characterize different sources and sinks of Si and their controlling geochemical processes. Several studies have shown that waters draining continents are enriched in heavy Si isotopes relative to source rocks, as secondary mineral formation during weathering preferentially incorporates light Si isotopes into newly formed clays e.g. (Georg et al., 2006; Cardinal et al., 2010; Cornelis et al., 2010; Hughes et al., 2011; Opfergelt et al., 2013; Fontorbe et al., 2013; Frings et al., 2014). In addition to this, seasonal variations in Si isotope ratios in river watersheds have been suggested to reflect either mixing of different water masses carrying distinct isotope ratios or biological activities, such as diatom production, that also fractionate Si isotopes (Ding et al., 2004; Alleman et al., 2005; Engström et al., 2010; Cardinal et al., 2010; Hughes et al., 2011; Cockerton et al., 2013; Sun et al., 2013). Decreasing $^{30}Si/^{28}Si$ ratios in rivers during high water discharge, such as during spring flood, suggest dissolution of Si-bearing clay minerals (Georg et al., 2006; Pokrovsky et al., 2013). Terrestrial plants and phytoliths also have relatively low $^{30}Si/^{28}Si$ ratios to DSi, which suggests that degradation of plant litter and phytoliths could provide an isotopically light Si pool to surface water during high water discharge (Hodson et al., 2008; Opfergelt et al., 2010; Cornelis et al., 2010; Pokrovsky et al., 2013; Frings et al., 2014). Until now, these processes have been studied in tropical, temperate and some boreal areas, but data in permafrost-covered polar areas are still scarce. This hinders the full understanding of Si cycling and land-sea Si fluxes in high-latitude systems.

The major river systems in the pan-arctic region act as integrators of the lithological and climatic changes across large watersheds, thus are ideal places to investigate the processes and the controlling factors of the Si-cycle in polar areas. In this study the Si dynamics in the Lena River watershed are investigated using stable Si isotopes. The Lena River has the ninth largest watershed in the world, of about $2.5 \times 10^6$ $km^2$, and is the second largest freshwater contributor, with a discharge of 581 $km^3$/yr transported to the Arctic Ocean via the Laptev Sea, following the Yenisey River discharge of 636 $km^3$/yr. The overall contribution of the Lena River to the Arctic Ocean is approximately 20% in terms of water discharge and major element fluxes (Holmes et al., 2011). The total DSi flux is 1 347 Gg Si/yr to the sea (Holmes et al., 2011), which is 12% of the total annual DSi flux in the pan-arctic area. The present study provides Si isotope-based data for the main channel of the Lena River as well as for a number of tributaries across the watershed among seasons. Si isotopes will shed light on major biogeochemical processes as weathering, clay formation and primary production patterns in such an extensive permafrost-dominated river system where impacts of increasing temperature on these fundamental processes are most drastic due to the polar amplification of climate change. The findings will also contribute to understanding present primary production and chemical cycles in the Arctic Ocean, and will establish a present-day baseline for quantifying changes in the future.

## 2. Materials and methods

### 2.1 Field sampling

River water samples were collected at 77 locations across the Lena River catchment during two field campaigns: July 2012 and June 2013. Seven monthly samples collected from September 2012 to March 2013 were also taken from the Lena River, at Yakutsk. An additional 9 spring flood samples were collected at the Tabaga Hydrological Station, 30 km south of Yakutsk during a field campaign between May 6$^{th}$ and 28$^{th}$, 2015. Among all the samples, 38 samples were collected in the main stream of the Lena River, and the remaining 55 samples were collected from tributaries (Figure 1). For the two major tributaries, the Aldan and Viliui Rivers, multiple samples were taken along their flow path over around 180 and 240 km, respectively. Samples were collected from the mouths of most of small tributaries, and in total 40 different tributaries were sampled. All sampling locations were localized using a GPS receiver (Garmin® 62). The pH, temperature and conductivity of the river waters were measured in the field. At each sampling location, a bottle of 50 ml sample was taken and filtered through pre-cleaned 142 mm diameter, 0.22 µm nitrocellulose membrane filters (Millipore®). The samples were acidified with HCl. Sampling details can be found in Hirst et al. (2017).

### 2.2 Major element analysis

The major cations and anions concentrations, including DSi, were measured by ICP-OES and ion chromatography (Thermo ICAP 6500 DUO and a Dionex, DX-120) with an accuracy of better than ± 5% measured from certified standards (NIST 1640a and in house multi element solutions).

### 2.3 Si isotope analysis

All samples were kept in dark for months to years, which allows certain amount of dissolved organic matter to degrade. Large amount of dissolved organic matter was also lost during the following procedure. Prior to Si isotope analysis, DSi was separated by adding a $MgCl_2$ solution to each sample for adjustment of the Mg concentration to 50 mM, sufficient for a two-step brucite co-precipitation that avoids incomplete Si recovery. By adding 1M NaOH the DSi was co-precipitated with $Mg(OH)_2$. The samples were then shaken for 30 min and left to settle for 12 hours prior to centrifugation. This was followed by adding an equal amount of 1 M NaOH to the supernatant and the same procedure was repeated. The DSi concentration in the supernatant was rechecked to assure the complete recovery of Si with precipitates (better than 97%). Details of the procedure can be found in Sun et al. (2014).

The chromatographic purification for Si recovered from dissolution of the precipitates was performed using ion exchange columns filled with a resin bed of 1.5 ml DOWEX 50W-X12 (200–400 mesh). This column setting was capable of effectively retaining Mg that was co-precipitated with Si. The purified Si was eluted with 18.2 Ωm Milli-Q water and stored for Si isotope analysis (Sun et al. 2014).

Silicon isotope analyses of water samples was performed using an MC-ICP-MS (Multicollector Inductively Coupled Plasma Mass Spectrometer), the Nu Plasma II (Nu Instruments, UK) at the Vegacenter, Swedish Museum of Natural History. A high mass resolution of 5000 allowed for a separation of the three Si ion beams from all major polyatomic interferences. The Si samples in 0.2 M HCl were introduced through a glass nebulizer (MicroMist, Glass Expansion) with an average uptake rate of 100 µl/minute. The

$^{28}$Si beam intensity was between 1.5 - 2 V/ppm. The $^{28}$Si background measured in pure 0.2 M HCl was lower than 50 mV and no background-induced effect on Si analysis was observed. The background was stable over days. For each full measurement (i.e. each reported Si isotope value of a sample), a standard-sample bracketing technique was applied. This included four individual measurements of the standard and three individual measurements of a sample in between. Each individual measurement consisted of forty cycles in two blocks.

Silicon isotope values are all reported in δ notation, which represents the parts per thousand (‰) deviation of the sample isotope ratio relative to that of the NBS28 standard, as follows:

$$\delta^{x}\mathrm{Si} = \left[\frac{({}^{x}Si/{}^{28}Si)_{sample}}{({}^{x}Si/{}^{28}Si)_{NBS28}} - 1\right] * 1000 \qquad \text{(Eq.1)}$$

where x=29 or 30. To ensure stability of the instrument and reproducibility of Si isotope analysis, four standards were regularly measured: (1) IRMM-18, a pure quartz standard, -1.79±0.06‰ ($2\sigma_{sd}$, n=11); (2) Big Batch, a highly fractionated $SiO_2$ material, -10.67±0.11‰ ($2\sigma_{sd}$, n=11); (3) Diatomite, a natural diatomite sample, +1.24±0.13‰ ($2\sigma_{sd}$, n=26); and (4) $ALOHA_{1000}$, a seawater standard that was recently established by the GEOTRACES seawater Si isotope intercalibration exercise, +1.21±0.08‰ (n=19), respectively. These values are in good agreement with earlier reported values (Reynolds et al., 2007; Grasse et al., 2017) and all measurements show mass-dependent fractionation of Si isotopes (Appendix Figure A1).

## 3. Results

### 3.1 The concentrations of DSi and $\delta^{30}Si_{DSi}$ values in the Lena River and its tributaries

The concentrations of ions in the Lena River and its tributaries sampled in July 2012 and June 2013 are summarized in Table 1. DSi concentrations in the Lena River and its tributaries ranged from 34 to 121 μM, with an average of 68 μM, while the $\delta^{30}Si_{DSi}$ values were between +0.39 to +1.71‰ with an average of +0.85‰, exhibiting variations of up to 1.32 ‰ in $\delta^{30}Si_{DSi}$ (Table 1 and Figure 3). There is a progressive increase in $\delta^{30}Si_{DSi}$ from +0.39±0.08 to +1.27±0.08‰ from south to north in the main stream of the Lena River, along with decreasing DSi concentrations from 87 to 58 μM from south to north. In contrast, DSi concentrations of tributaries in the Verkhoyansk Mountain Range increased from 45 to 85 μM from south to north, with $\delta^{30}Si_{DSi}$ values ranging from +0.39±0.08 to +1.48±0.12‰. DSi concentrations and $\delta^{30}Si_{DSi}$ values from the Aldan and Viliui Rivers were relatively uniform, around 78 and 66 μM, for DSi and +0.51±0.05 and +1.33±0.1 ‰, for $\delta^{30}Si_{DSi}$, respectively. The maximum value of DSi concentration, 121 μM, was from in the Central Siberian Plateau, while the peak $\delta^{30}Si_{DSi}$ value, +1.71±0.08‰, was found in the Lena-Amganski Inter-River area.

### 3.2 The DSi concentrations and $\delta^{30}Si_{DSi}$ values, in the Lena River, during the winter and the spring flood time series

Alkalinity, DSi concentrations and the $\delta^{30}Si_{DSi}$ values all exhibited large variations from summer to winter 2012-2013 (Table 2 and Figure 4). Alkalinity ranged from 1.2 to 3.3 mM and DSi concentrations increased from 74 μM in autumn to 172 μM in winter. The corresponding $\delta^{30}Si_{DSi}$ values varied from +1.17±0.09 to +1.65±0.09‰. During the spring flood in 2015, alkalinity decreased significantly from 1.7 to 0.58 μM and DSi concentrations declined from 79 to 53 μM. The $\delta^{30}Si_{DSi}$ values also decreased from +1.04±0.08‰ at the beginning of the flood to +0.58±0.09‰ at the end of the flood.

## 4. Discussion

### 4.1 DSi concentrations and $\delta^{30}Si_{DSi}$ values of the Lena River watershed

The average DSi concentration is 68 μM in the Lena River watershed, which is less than half of the typical global river water concentration of 160 μM (Beusen et al., 2009; Dürr et al., 2011). This is consistent with an underlying global pattern of climate control on silicate weathering. Lower concentrations are usually observed in cold high-latitude systems, while the tropical areas tend to have higher concentrations. The average $\delta^{30}Si_{DSi}$ value of the Lena River including values from its tributaries is +0.87‰, which is similar to published $\delta^{30}Si_{DSi}$ values in global rivers. The tropical rivers such as the Amazon River and the Congo River have an average $\delta^{30}Si_{DSi}$ values of +0.92‰ and +0.98‰, respectively (Cardinal et al., 2010; Hughes et al., 2013). Temperate alpine rivers have shown $\delta^{30}Si_{DSi}$ values in a range of +0.4 to +1.2‰ (De La Rocha et al., 2000; Georg et al., 2006), while somewhat higher values of +0.49 to +2.71‰ have been reported in the Ganges draining the Himalaya and its alluvial plain, with a range of +0.81 to +3.04‰ (Fontorbe et al., 2013; Frings et al., 2015). Similarly, $\delta^{30}Si_{DSi}$ values of +0.7 to +3.4‰ have been observed in the temperate Yangtze River (Ding et al., 2004). The boreal but permafrost-free Kalix River located in northern Sweden has $\delta^{30}Si_{DSi}$ values of between +0.7 and +1.5‰ (Engström et al., 2010). Central Siberian rivers located in permafrost areas at similar latitudes to that of the Lena River were reported to have a $\delta^{30}Si_{DSi}$ range of +1.08 to +1.67‰, with peaks in summer of between +1.5 and +2.5‰

(Pokrovsky et al., 2013). $\delta^{30}Si_{DSi}$ values of the Yenisey River and its tributaries have ranged from +0.75 to +2.11‰ during spring flood (Mavromatis et al., 2016).

Overall, rivers across the Arctic region show similar variations in $\delta^{30}Si_{DSi}$ values as in rivers draining other climate regimes. Their $\delta^{30}Si_{DSi}$ values are higher than those of primary silicate minerals with a range from -1.1 to +0.7‰ (Basile-Doelsch et al., 2005; Savage et al., 2011; Opfergelt and Delmelle, 2012). The differences between $\delta^{30}Si_{DSi}$ values of primary minerals and rivers have been interpreted to reflect Si isotope fractionation during silicate weathering (Georg et al., 2006; Cardinal et al., 2010; Hughes et al., 2011; Fontorbe et al., 2013; Frings et al., 2014). Seasonal variations of water discharge carrying different DSi concentrations, however, are subsequently superimposed on the weathering signal, and reflect fractionation by biological activity (exclusively by vascular plants and diatoms) or mixing of waters with different end-member compositions (such as between groundwater and surface water).

## 4.2 Processes controlling $\delta^{30}Si_{DSi}$ values in the Lena River watershed

Variations of $\delta^{30}Si_{DSi}$ values both in the Lena River and the tributaries reflect the cumulative effects of many processes. Therefore, it is often difficult to distinguish various processes from each other given our limited data collected over such a huge watershed. Here, we discuss the most important processes and attempt to distinguish the dominant process that leads to Si isotope fractionation in different areas of the Lena River watershed.

### 4.2.1 Main channel of the Lena River

In general, the $\delta^{30}Si_{DSi}$ values increase toward the north corresponding with decreasing DSi concentrations in the Lena River main channel. This could be caused either by a kinetic process that preferably take up lighter Si isotopes during consumption of DSi or simply by mixing with tributaries with lower DSi concentrations and higher $\delta^{30}Si_{DSi}$ values.

To assess the degree of Si isotope fractionation, the Rayleigh model is chosen (Eq. 2). When DSi from a locally well-mixed water is incrementally removed by a kinetic process, the Si isotope values of DSi in the water is related to the extent of DSi depletion as expressed by:

$$\delta^{30}Si_{DSi} = \delta^{30}Si_0 + \varepsilon ln(f) \qquad \text{Eq. 2}$$

Or Eq. 2 could be rearranged as

$$\delta^{30}Si_{DSi} = \delta^{30}Si_0 + \varepsilon ln(\frac{[DSi]}{[DSi_0]}) = \delta^{30}Si_0 - \varepsilon ln([DSi_0]) + \varepsilon ln([DSi]) \quad \text{Eq. 3}$$

where $\delta^{30}Si_{DSi}$ and $\delta^{30}Si_0$ are the Si isotope values of remaining DSi in water and initial DSi, respectively. Si isotope fractionation is represented by $\varepsilon = (\alpha - 1) \times 1000$, where the Si isotope fractionation factor is $\alpha = (^{30}Si/^{28}Si)_{Solid} / (^{30}Si/^{28}Si)_{Diss}$ . The variable $f$ is the ratio of remaining to initial DSi concentration (i.e. $\frac{[DSi]}{[DSi_0]}$), where the remaining DSi is the DSi concentration measured in river samples. The upstream of the Lena River and the Aldan River have similar $\delta^{30}Si_{DSi}$ values, which could serve as one endmember, i.e. $\delta^{30}Si_0$ assuming to be +0.38‰. Figure 2A shows that the $\delta^{30}Si_{DSi}$ values of the Lena River main channel follow the Rayleigh model well ($R^2$=0.87). The regression lines give $\varepsilon$ of -1.40‰. $DSi_0$ is estimated to be 85 µM by resolving the intercept, $\delta^{30}Si_0 - \varepsilon ln([DSi_0])$, in Eq. 3.

The Si isotope fractionation observed by the Rayleigh model likely reflects strong biological activity (e.g. diatom production) because: 1) the $\varepsilon$ value is in agreement with the values estimated from laboratory studies (De La Rocha et al., 1997; Sutton et al., 2013; Sun et al.,

2014) and field studies of freshwater and marine diatom production (De La Rocha et al., 2000; Alleman et al., 2005; Fripiat et al., 2011; Opfergelt et al., 2011); 2) a number of diatoms have been widely observed in the filter samples (Hirst et al., 2017); 3) no clear patterns have been revealed between $\delta^{30}Si_{DSi}$ and the concentration ratio of DSi to cations, indicating a minor role of weathering and secondary clay formation.

The biological process can be represented by a steady-state model, in which production is at steady state with a constant supply from external sources. However, in this study, the Rayleigh model is used given the physical scenario in the river it would reflect. The Rayleigh model shows the compositions for waters that are subject to different degrees of DSi removal ($f$) from water with a single starting composition, i.e. $\delta^{30}Si_{DSi}$ would change with different $f$ values starting from a single $\delta^{30}Si_0$ value. This reflects the progressive DSi depletion in the Lena River.

Beside biological activities, simultaneously there is also mixing between a number of tributaries and the Lena River main channel, as well as mixing within the main channel of waters that have suffered varying degrees of depletion by biological production. If there are major tributaries with lower DSi concentrations and higher $\delta^{30}Si_{DSi}$ values then these could be responsible for decreases of DSi concentrations in the Lena River main channel. Further, Bouchez et al. (2010) have suggested that the confluence of two water masses in large rivers can take tens to hundreds of kilometers, i.e. incomplete mixing could be observed. The $\delta^{30}Si_{DSi}$ values of the two main tributaries, the Aldan and Viliui Rivers are also plotted in Figure 2A, as one would expect the largest mixing to occur between these two tributaries and the main channel. The Aldan River shares similar DSi concentrations and $\delta^{30}Si_{DSi}$ values with upstream of the Lena River, and so could not lead to higher $\delta^{30}Si_{DSi}$ values in the main channel. This means that the Aldan River is likely to serve together with the upstream of the Lena River as an endmember prior to biological production or strong mixing in the downstream. The Viliui River with higher $\delta^{30}Si_{DSi}$ values only contributes <10% of DSi load to the Lena River main channel (Kutscher et al., 2017), implicating the fast confluence of the Viliui River and the Lena main channel. Mixing between the Viliui River and the Lena main channel only leads to the $\delta^{30}Si_{DSi}$ value of around +0.5‰ if one takes +0.4‰ of the Lena upstream and +1.2‰ of the Viliui River as two endmembers. The $\delta^{30}Si_{DSi}$ values of the Viliui Rivers stand out from the Rayleigh and mixing line of the Lena River confirms the minor role of Viliui mixing into the Lena River. Contributions from other tributaries are even smaller than the Viliui River and are considered to be negligible.

To evaluate the impact of the mixing, and an example is shown in Figure 2A where water from tributaries with an $\delta^{30}Si_{DSi}$ value of +0.40‰ and $f$=0.90 (i.e. similar to water from upstream of the Lena River) mixes with water with a higher $\delta^{30}Si_{DSi}$ value of +1.03‰ and $f$=0.65 (i.e. water from downstream of the Lena River that has suffered Si depletion due to biological activity). Resulting mixtures with different contributions of the two waters fall on a mixing line that does not significantly deviate from the Rayleigh model line (Figure 2A). This indicates that mixing does not obscure the signal of DSi depletion by biological production (given a wide range of values derived from the biological depletion) and some intermediate values may to some extent reflect mixing. While adding DSi along the Lena River with average $\delta^{30}Si_{DSi}$ values that are the same as the $\delta^{30}Si_0$ value would move the $\delta^{30}Si_{DSi}$ values in the Lena River back towards the initial value, biological activity would still be the cause of lower DSi concentrations and higher $\delta^{30}Si_{DSi}$ values.

Some recent studies have shown small but measurable Si isotope fractionations during biogenic silica dissolution, with the lighter Si isotopes preferentially released to DSi during dissolution with a value for $\varepsilon$ of -0.55‰ for marine diatoms (Demarest et al., 2009) and -0.86‰ for estuarine diatoms (Sun et al., 2014), whereas no isotope fractionations were observed using sedimentary diatom opal (Wetzel et al., 2014). Whether or not Si isotopes are fractionated during dissolution remain unclear. Despite this, this process is not likely to be important in the Lena River, as active diatom production in summer greatly surpasses dissolution and Si isotope fractionation from dissolution of biogenic silica will be restricted.

**4.2.2 Verkhoyansk mountain range**

For the tributaries draining the Verkhoyansk mountain range, the observed range of $\delta^{30}Si_{DSi}$ values from +0.39 to +1.48‰ is different from the trend in the Lena River (Figure 2B). A broad correlation between reciprocal DSi concentrations and $\delta^{30}Si_{DSi}$ values are observed ($R^2$=0.30, p<<0.05, Figure 3A). This correlation suggests that $\delta^{30}Si_{DSi}$ values increase in mountainous areas with elevated DSi concentrations and this is most likely caused by the extent of silicate weathering. A correlation between $\delta^{30}Si_{DSi}$ values and Na*+K concentrations (Na*+K = Na – Cl + K for the evaporite correction, $R^2$=0.32) shows relative removal of DSi to Na and K and the loss of lighter Si isotopes (Figure 3B), suggesting secondary clay formation during silicate weathering.

The Si isotope weathering signal is consistent with incorporation of Si in secondary clays formed during weathering. Lighter Si isotopes are incorporated into newly formed clays, leaving DSi enriched with heavier Si isotopes. This has been demonstrated for a laboratory-controlled early stage experiment of clay formation (Oelze et al., 2014). Studies based on Si isotopes in river systems have invoked clay formation to explain similar $\delta^{30}Si_{DSi}$ variations, such as in the Nile River (Cockerton et al., 2013), the Congo River (Cardinal et al., 2010), the Scheldt River (Delvaux et al., 2013) and central Siberia rivers (Pokrovsky et al., 2013). The reported lower $\delta^{30}Si$ values in clay minerals ranging from -2.95 to -0.16‰ have also supported our observations (Cornelis et al., 2010; Douthitt, 1982; Opfergelt et al., 2010; Ziegler et al., 2005). An earlier study by Georg et al. (2006) suggested the use of Al/Si ratios as tracers for this process, as clay formation removes Al relative to Si and low Al/Si ratios are then associated with high $\delta^{30}Si_{DSi}$ values. Figure 3C does not reveal any significant correlation between Al/Si ratios and $\delta^{30}Si_{DSi}$ values although $\delta^{30}Si_{DSi}$ values display large variations with decreasing Al/Si ratios. pH is another factor that controls Al speciation, but it is not likely the reason for the insignificant correlation, as variations in pH among these tributaries ranging from 6.3 to 7.6 while Al speciation is mainly observed below pH 4.5. The Lena River has high concentrations of dissolved organic carbon, ranging from 590 to 1300 μM during our sampling period (Kutscher et al. 2017), thus organic acids could also be an important factor. Al has been shown to highly bound with organic carbon in a Siberian river (Pourpoint et al., 2017), thus preventing the formation of clay minerals which precipitates Al (Pokrovsky et al., 2016). Similarly, due to the low solubility of Al, the formation of colloidal gibbsite can also remove Al from solution. These processes could be particularly important in permafrost-covered watersheds like the Lena River where organic carbon is released during spring-summer thawing of permafrost.

The detailed Si isotope fractionation mechanisms during clay formation also remain poorly studied, partly because clay formation is not a single process with a fixed isotope fractionation factor and so hard to synthesise in the lab (Opfergelt and Delmelle, 2012) and partly because of the dynamics of repeated cycles of dissolution and re-precipitation (Basile-Doelsch et al., 2005; Cornelis et al., 2014). Furthermore, this is also complicated by different clay minerals exhibiting different Si isotope fractionation factors among different clay minerals (Opfergelt and Delmelle, 2012). Opfergelt and Delmelle (2012) report that the Si isotope fractionation factors between primary minerals and clays can vary between -2 and -1‰, which is consistent with the observed range of $\delta^{30}Si_{DSi}$ values in the Verkhoyansk mountain range. The $\delta^{30}Si_{DSi}$ values from +0.39 to +1.48‰ integrate the DSi flows from each tributary and to a large extent reflect the degree of weathering in the Verkhoyansk mountain range.

Temperature is known to be an important factor controlling weathering rates (Kump et al., 2000; Li et al., 2016). Surface water draining warmer areas have higher $\delta^{30}Si_{DSi}$ values and major ion concentrations compared to cooler areas given their different weathering rates. In the Verkhoyansk mountain range, Figure 3D ($R^2$=0.51, p<<0.05) suggests a marked temperature impact on the weathering in these high-latitude mountain areas, but this correlation might be obscured as temperatures were measured at the river mouths of tributaries but not in the weathering zones. Another reason for this observed correlation could be glacial influence, as the slope and water discharge of rivers on high mountains increase with decreased temperature. This means that more particulate suspended matters are flushed into rivers under lower temperature, which may shift $\delta^{30}Si_{DSi}$ values to lower values by dissolution of isotopically light silicate minerals at high fluid : solid ratios (Georg et al. 2006).

#### 4.2.3 Central Siberian Plateau and Lena-Amganski Inter-River Area

Terrestrial biological production also discriminate against the heavier Si isotopes during uptake at the root-interface in soils (Opfergelt et al., 2006; Ding et al., 2008; Delvigne et al., 2009), and consequently enrich the soil solutions with heavier Si isotopes. This is likely the reason for higher $\delta^{30}Si_{DSi}$ values observed in tributaries in Central Siberian Plateau and Lena-Amganski Inter-River Area, which flush through soils (Figure 2B). The range of $\delta^{30}Si_{DSi}$ values in these areas is large, with values from +0.52 to +1.71‰ that reflect different Si isotope fractionations from the original Si sources to the rivers. This can be explained at least partially by an effect of different vascular plant species (Opfergelt et al., 2006) and their growth stage (Ding et al., 2008) given the Si isotope fractionation factor of -1‰ during their production (Opfergelt and Pierre, 2012; Frings et al. 2016) and approximately half of terrestrial net primary production by Si accumulating organisms (Carey and Fulweiler, 2012). Another reason could be secondary clay formation in soil solutions during basalt weathering in Central Siberian Plateau (Pokrovsky et al. 2005). This indicates that the $\delta^{30}Si_{DSi}$ values in the tributaries possibly carry both strong terrestrial production and weathering signal, which is different from those in the Lena River. However, lack of clear correlations between $\delta^{30}Si_{DSi}$ values and DSi concentrations in these two areas suggest other processes complicate the overall pattern of $\delta^{30}Si_{DSi}$ distribution and it is not possible to distinguish those processes that control Si. Hence, the $\delta^{30}Si_{DSi}$ values in tributaries may serve as an integrated value for the Central Siberian Plateau and Lena-Amganski Inter-River Area.

### 4.3 Seasonal variations in the upstream of the Lena River

Figure 4A displays annual variations of $\delta^{30}Si_{DSi}$ values with an average value of +1.6‰ during winter, October 2012 to March 2013 and Figure 4B shows the sharp drop of $\delta^{30}Si_{DSi}$

values down to +0.63‰ during the rapid transition from the winter water flow to the spring flood in May 2015. The values decrease by nearly 1‰ from winter to spring, which coincides with the water discharge maximum, i.e. snowmelt in the Lena River watershed. The winter baseflow, dominated by groundwaters with high $\delta^{30}Si_{DSi}$ values, is diluted by the large amount of snowmelt water that flush through soils carrying low $\delta^{30}Si_{DSi}$ values during the spring flood. Figure 5A shows the $\delta^{30}Si_{DSi}$ values *vs* 1/DSi for the entire temporal period with $R^2$=0.84, possibly reflecting mixing of two distinct water bodies. The $\delta^{30}Si_{DSi}$ values during the spring flood in May 2015 remain almost constant and its average value can serve as one endmember of $\delta^{30}Si_{DSi}$ values in the Lena River. The other end-member has higher DSi concentration and a higher $\delta^{30}Si_{DSi}$ value than the average winter $\delta^{30}Si_{DSi}$ value of +1.6‰, but lower than +2.3‰ (given by the intercept of the regression line; Figure 5A). This implies a pronounced DSi supply and Si isotope fractionation in upstream of Yakutsk in the Lena River throughout the year, which implies strong secondary clay mineral formation during weathering in intrapermafrost groundwater in winter, as lighter Si isotopes are preferably incorporated into clay minerals, leaving heavier Si isotopes in water.

As suggested by Georg et al (2006), a plot of $\delta^{30}Si_{DSi}$ values vs dissolved Al/Si could reveal the impact of clay formation and its potential for fractionating Si isotopes. Figure 5B displays a linear correlation between $\delta^{30}Si_{DSi}$ values vs Al/Si in the spring flood ($R^2$=0.69, $p<<0.05$). Without clay formation, the $\delta^{30}Si_{DSi}$ values are expected to reflect the isotopic composition of primary silicates ($\delta^{30}Si$ = -0.4‰, Frings et al. 2016), and using the data correlation this corresponds to an Al/Si ratio of 0.22. Decreasing Al/Si ratios in river water corresponds to increased $\delta^{30}Si_{DSi}$ values, indicating a faster removal of Al compared to Si, and preferential uptake of lighter Si isotopes into newly formed clays. Extrapolation of the data to Al/Si=0 gives the intercept of $\delta^{30}Si$ = +0.96‰ and corresponds to complete removal of and so the highest $\delta^{30}Si_{DSi}$ value created in waters for secondary clay formation during weathering. During winter (October to March), the surface soils in the Lena River watershed are frozen, which restricts the major transport processes in soils but increases the residence and contact time between intrapermafrost groundwaters and the frozen pemafrost soils and bedrock. Thus the winter $\delta^{30}Si_{DSi}$ values are likely to represent $\delta^{30}Si_{DSi}$ values in groundwater and range between +1.32 and +1.86‰. This agrees with the scenario suggested for central Siberian rivers, which exhibits the winter $\delta^{30}Si_{DSi}$ values in between +1.0 to +2.5‰ (Pokrovsky et al., 2013).

During snowmelt the high water discharge causes water flushing through the upper soils, which is observed by a simultaneous increase in dissolved organic carbon concentrations in the river (Kutscher et al. 2017). High water discharge also includes leached water from the upper soil profile and is likely to carry lighter $\delta^{30}Si_{DSi}$ values due to mobilization of DSi released from dissolution of silicate materials and dissolution of plant phytoliths in large rivers (Ding et al., 2004; Ziegler et al., 2005; Pokrovsky et al., 2005; Georg et al., 2006; Pokrovsky et al., 2013). Analyses of soil porewaters during the spring flood in northern Sweden (boreal, but not underlain by permafrost) indicates that these waters contribute approximately 90% of the total Si in river water, while groundwater does not supply more than 15% (Land et al., 2000). Thus, contributions of soil floor leachates to river water during the spring flood is expected to dominate in boreal river systems and likely the Lena River as well. This suggests that soil solutions are very likely to have $\delta^{30}Si_{DSi}$ value similar to the average $\delta^{30}Si_{DSi}$ value of +0.6‰ observed in the Lena River during the spring flood.

**4.4 Implications for Si isotope flux to the Arctic Ocean**

The $\delta^{30}Si_{DSi}$ values in the Lena River and its tributaries vary between +0.39 to +1.86‰. The spring flood has a $\delta^{30}Si_{DSi}$ value of +0.6‰ and this value increases to +1.3‰ downstream of the Lena River during summer and increases to peak values of +1.86‰ in winter. Tributaries with various Si sources contribute to this range during the mixing with the main channel. This suggests that there is a dynamic shift seasonally between sources and processes and this shift is the primary controlling factor of DSi and $\delta^{30}Si_{DSi}$ values in the Lena River and ultimately the Si export to the Arctic Ocean. Long-term water discharge and DSi concentrations are available via Arctic Great Rivers Observatory (http://www.arcticgreatrivers.org/data.html). By using a 5-year average for the water discharge and DSi concentrations from 2010-2014 (Appendix Table A1, but no Si data available for 2015) in the Lena River main channel, which are representative for our sampling periods 2012, 2013 and 2015, a Si flux-weighted annual $\delta^{30}Si_{DSi}$ value is calculated to be +0.86±0.3‰. This calculation is based on the average $\delta^{30}Si_{DSi}$ values from spring, summer and winter samples in this study, +0.6, +0.8 and +1.6‰, respectively, and the contributions of spring, summer and winter Si discharges to the total annual Si flux, 26, 60 and 14%, respectively.

The Yenisey River has the $\delta^{30}Si_{DSi}$ value of +1.6±0.25‰, which was calculated using measured spring flood $\delta^{30}Si_{DSi}$ value of +1.3‰, summer $\delta^{30}Si_{DSi}$ value of +1.5 ‰ derived from Central Siberian rivers and winter $\delta^{30}Si_{DSi}$ value of +2.0‰ adopted from the Nizhnaya Tunguska River (Mavromatis et al., 2016). These values are all higher than the Lena River values measured in this study, which is possibly caused by higher degree of formation of secondary clay minerals and stronger biological activities during summer. However, there are uncertainties associated with our calculations for the Lena River including: 1) the contributions from the Lena tributaries and especially for tributaries with higher $\delta^{30}Si_{DSi}$ values in summer are not included in the calculation because of the lack of water discharge data. Therefore, the average $\delta^{30}Si_{DSi}$ value in summer is likely underestimated. 2) The isotope values used in the calculation are not from samples of the river mouth, with some from around Yakutsk (e.g. spring flood samples and some samples from upstream of the Lena River main channel); hence certain variations of $\delta^{30}Si_{DSi}$ caused by biological activity in the river and mixing with tributaries in the downstream should be expected along the water flow path from the upstream to the river mouth.

## 5. Conclusions

Our results cover almost an annual cycle of variations in DSi and $\delta^{30}Si_{DSi}$ values in the Lena River, Siberia, and there is a general trend with lower $\delta^{30}Si_{DSi}$ values associated with high DSi flux and higher $\delta^{30}Si_{DSi}$ values associated with low DSi flux. This is similar to observations in other large river systems, including Amazon, Congo and Yenisey and confirms that there is a hydrological control of the Si isotope compositions delivered to the ocean irrespectively of climate zones.

The results reveal a large variation in the $\delta^{30}Si_{DSi}$ values both geographically and temporally. The $\delta^{30}Si_{DSi}$ values in summer range between +0.39 to +1.71‰, and are caused both by mixing of tributaries with various $\delta^{30}Si_{DSi}$ values and biological uptake of DSi through vascular plant and phytoplankton growth on land and in rivers. Secondary clay mineral formation may also play an important role by the enrichment of DSi with heavier Si isotopes in soil- and intrapermafrost groundwater, resulting in higher $\delta^{30}Si_{DSi}$ values in the tributaries.

Subsequently this will increase the $\delta^{30}Si_{DSi}$ values of the water discharge to the main stream and possibly further interact with river sediments. From winter to spring, the $\delta^{30}Si_{DSi}$ in the Lena River decreases temporally from high values in winter to low values during the spring flood with high discharge. This is likely caused by a change in the dominant source for Si from permafrost-hosted deep intrapermafrost groundwater during winter to dissolution of silicate materials and phytoliths from the active upper soil layers as well as suspended materials from the bank abrasion during spring discharge.

The annual $\delta^{30}Si_{DSi}$ value of the Si flux to the Arctic Ocean is calculated to be +0.86±0.3‰, which is lower than +1.6±0.25‰ as reported for the Yenisey River. These two rivers are responsible for nearly half of the dissolved Si delivered to the Arctic Ocean and the grand Si inputs to the Arctic Ocean carry an average $\delta^{30}Si_{DSi}$ value of +1.3±0.3‰ based weighted Si flux of these two rivers. Global warming not only promotes chemical weathering associated with permafrost thawing and hydrological regime change, but also results in the vegetation rise and colonization of the northernmost territory, all of which would remove isotopically-light DSi and shift $\delta^{30}Si_{DSi}$ values towards higher values in soils and groundwater and their discharges to river water.

**Acknowledgements**

This project was supported by the Swedish Research Council (VR 621-2010-3917) and the Swedish Polar Research Secretariat (SIMO 2011-165 and 2012-213). Special thanks to our Russian colleagues and the crews on R/V “Akademik” and “Merelotoved”. This is contribution #xx from the Vegacenter.

## References


Alleman L. Y., Cardinal D., Cocquyt C., Plisnier P.-D., Descy J.-P., Kimirei I., Sinyinza D. and André L. (2005) Silicon Isotopic Fractionation in Lake Tanganyika and Its Main Tributaries. *J. Great Lakes Res.* **31**, 509–519.

Basile-Doelsch I., Meunier J. D. and Parron C. (2005) Another continental pool in the terrestrial silicon cycle. *Nature* **433**, 399–402.

Beusen A. H. W., Bouwman A. F., Dürr H. H., Dekkers A. L. M. and Hartmann J. (2009) Global patterns of dissolved silica export to the coastal zone: Results from a spatially explicit global model. *Global Biogeochem. Cycles* **23**, GB0A02, doi:10.1029/2008GB003281.

Cardinal D., Gaillardet J., Hughes H. J., Opfergelt S. and André L. (2010) Contrasting silicon isotope signatures in rivers from the Congo Basin and the specific behaviour of organic-rich waters. *Geophys. Res. Lett.* **37**, L12403, doi:10.1029/2010GL043413.

Cockerton H. E., Street-Perrott F. A., Leng M. J., Barker P. A., Horstwood M. S. A. and Pashley V. (2013) Stable-isotope (H, O, and Si) evidence for seasonal variations in hydrology and Si cycling from modern waters in the Nile Basin: implications for interpreting the Quaternary record. *Quat. Sci. Rev,* **66**, 4–21.

Cornelis J. T., Delvaux B., Cardinal D., André L., Ranger J. and Opfergelt S. (2010) Tracing mechanisms controlling the release of dissolved silicon in forest soil solutions using Si isotopes and Ge/Si ratios. *Geochim. Cosmochim. Acta* **74**, 3913–3924.

Cornelis J. T., Delvaux B., Georg R. B., Lucas Y., Ranger J. and Opfergelt S. (2011) Tracing the origin of dissolved silicon transferred from various soil-plant systems towards rivers: a review. *Biogeosciences* **8**, 89–112.

Cornelis J.-T., Weis D., Lavkulich Les, Vermeire M.-L., Delvaux B. and Barling J. (2014) Silicon isotopes record dissolution and re-precipitation of pedogenic clay minerals in a podzolic soil chronosequence. *Geoderma* **235-236**, 19–29.

De La Rocha De C. L., Brzezinski M. A. and DeNiro M. J. (2000) A first look at the distribution of the stable isotopes of silicon in natural waters. *Geochim. Cosmochim. Acta* **64**, 2467–2477.

De La Rocha De C. L., Brzezinski M. A. and DeNiro M. J. (1997) Fractionation of silicon isotopes by marine diatoms during biogenic silica formation. *Geochim. Cosmochim. Acta* **61**, 5051–5056.

Delvaux C., Cardinal D., Carbonnel V., Chou L., Hughes H. J. and André L. (2013) Controls on riverine δ30Si signatures in a temperate watershed under high anthropogenic pressure (Scheldt — Belgium). *J Mar. Syst.* **128**, 40–51.

Delvigne C., Opfergelt S., Cardinal D., Delvaux B. and André L. (2009) Distinct silicon and germanium pathways in the soil-plant system: Evidence from banana and horsetail. *J. Geophys. Res.* **114**, G02013. doi:10.1029/2008JG000899

Demarest M. S., Brzezinski M. A. and Beucher C. P. (2009) Fractionation of silicon isotopes during biogenic silica dissolution. *Geochim. Cosmochim. Acta* **73**, 5572–5583.

Ding T. P., Tian S. H., Sun L., Wu L. H., Zhou J. X. and Chen Z. Y. (2008) Silicon isotope fractionation between rice plants and nutrient solution and its significance to the study of the silicon cycle. *Geochim. Cosmochim. Acta* **72**, 5600–5615.

Ding T., Wan D., Wang C. and Zhang F. (2004) Silicon isotope compositions of dissolved silicon and suspended matter in the Yangtze River, China. *Geochim. Cosmochim. Acta* **68**, 205–216.

Dürr H. H., Meybeck M., Hartmann J., Laruelle G. G. and Roubeix V. (2011) Global spatial distribution of natural riverine silica inputs to the coastal zone. *Biogeosciences* **8**, 597–620.

Engström E., Rodushkin I., Ingri J., Baxter D. C., Ecke F., Österlund H. and Öhlander B. (2010) Temporal isotopic variations of dissolved silicon in a pristine boreal river. *Chem. Geol.* **271**, 142–152.

Fontorbe G., De La Rocha C. L., Chapman H. J. and Bickle M. J. (2013) The silicon isotopic composition of the Ganges and its tributaries. *Earth Planet. Sci. Lett* **381**, 21–30.

Frey K. E. and McClelland J. W. (2009) Impacts of permafrost degradation on arctic river biogeochemistry ed. T. D. Prowse. *Hydrol. Process.* **23**, 169–182.

Frings P. J., Clymans W., Fontorbe G., Gray W., Chakrapani G. J., Conley D. J. and De La Rocha C. (2015) Silicate weathering in the Ganges alluvial plain. *Earth Planet. Sci. Lett* **427**, 136–148.

Frings P. J., Clymans W., Fontorbe G., De La Rocha C. L. and Conley D. J. (2016) The continental Si cycle and its impact on the ocean Si isotope budget. *Chem. Geol.* **425**, 12–36.

Frings P. J., De La Rocha C., Struyf E., van Pelt D., Schoelynck J., Hudson M. M., Gondwe M. J., Wolski P., Mosimane K., Gray W., Schaller J. and Conley D. J. (2014) Tracing silicon cycling in the Okavango Delta, a sub-tropical flood-pulse wetland using silicon isotopes. *Geochim. Cosmochim. Acta* **142**, 132–148.

Fripiat F., Cavagna A.-J., Savoye N., Dehairs F., André L. and Cardinal D. (2011) Isotopic constraints on the Si-biogeochemical cycle of the Antarctic Zone in the Kerguelen area (KEOPS). *Mar. Chem.* **123**, 11–22.

Georg R. B., Reynolds B. C., FRANK M. and Halliday A. N. (2006) Mechanisms controlling the silicon isotopic compositions of river waters. *Earth Planet. Sci. Lett* **249**, 290–306.

Grasse P., Brzezinski M. A., Cardinal D., de Souza G. F., Andersson P., Closset I., Cao Z., Dai M., Ehlert C., Estrade N., Francois R., Frank M., Jiang G., Jones J. L., Kooijman E., Liu Q., Lu D., Pahnke K., Ponzevera E., Schmitt M., Sun X., Sutton J. N., Thil F., Weis

D., Wetzel F., Zhang A., Zhang J. and Zhang Z. (2017) GEOTRACES inter-calibration of the stable silicon isotope composition of dissolved silicic acid in seawater. *J. Anal. At. Spectrom.*, 1–45.

Grasse P., Ryabenko E., Ehlert C., Altabet M. A. and Frank M. (2016) Silicon and nitrogen cycling in the upwelling area off Peru: A dual isotope approach. *Limnol. Oceanogr.* **61**, 1661–1676.

Hirst C., Andersson P. S., Shaw S., Burke I. T., Kutscher L., Murphy M. J., Maximov T., Pokrovsky O. S., Mörth C.-M. and Porcelli D. (2017) Characterisation of Fe-bearing particles and colloids in the Lena River basin, NE Russia. *Geochim. Cosmochim. Acta*. doi.org/10.1016/j.gca.2017.07.012

Hodson M. J., Parker A. G., Leng M. J. and Sloane H. J. (2008) Silicon, oxygen and carbon isotope composition of wheat (Triticum aestivum L.) phytoliths: implications for palaeoecology and archaeology. *J. Quaternary Sci.* **23**, 331–339.

Holmes R. M., McClelland J. W., Peterson B. J., Tank S. E., Bulygina E., Eglinton T. I., Gordeev V. V., Gurtovaya T. Y., Raymond P. A., Repeta D. J., Staples R., Striegl R. G., Zhulidov A. V. and Zimov S. A. (2011) Seasonal and Annual Fluxes of Nutrients and Organic Matter from Large Rivers to the Arctic Ocean and Surrounding Seas. *Estuaries and Coasts* **35**, 369–382.

Hughes H. J., Sondag F., Cocquyt C., Laraque A., Pandi A., André L. and Cardinal D. (2011) Effect of seasonal biogenic silica variations on dissolved silicon fluxes and isotopic signatures in the Congo River. *Limnol. Oceanogr.* **56**, 551–561.

Hughes H. J., Sondag F., Santos R. V., André L. and Cardinal D. (2013) The riverine silicon isotope composition of the Amazon Basin. *Geochim. Cosmochim. Acta* **121**, 637–651.

Kump L. R., Brantley S. L. and Arthur M. A. (2000) Chemical weathering, atmospheric CO2 and climate. *Annu. Rev. Earth Planet. Sci.* **28**, 611–667.

Kutscher L., Mörth C.-M., Porcelli D., Hirst C., Maximov T. C., Petrov R. E., Andersson P. S. Spatial variation in concentration and sources of organic carbon in the Lena River, Siberia. *J. Geophys. Res.: Biogeosciences,* **122,** 8, 1999-2016.

Land M., Ingri J., Andersson P. S. and Öhlander B. (2000) Ba/Sr, Ca/Sr and $^{87}Sr/^{86}Sr$ in soil water and groundwater: implications for relative contributions to stream water discharge. *Appl. Geochem.* **15**, 311–325.

Li G., Hartmann J., Derry L. A., West A. J., You C.-F., Long X., Zhan T., Li L., Li G., Qiu W., Li T., Liu L., Chen Y., Ji J., Zhao L. and Chen J. (2016) Temperature dependence of basalt weathering. *Earth Planet. Sci. Lett* **443**, 59–69.

Ma X., Yasunari T., Ohata T. and Fukushima Y. (2005) The influence of river ice on spring runoff in the Lena river, Siberia. *Annals of Glaciology* **40**, 123–127.

Mavromatis V., Rinder T., Prokushkin A. S., Pokrovsky O. S., Korets M. A., Chmeleff J. and Oelkers E. H. (2016) The effect of permafrost, vegetation, and lithology on Mg and Si isotope composition of the Yenisey River and its tributaries at the end of the spring flood. *Geochim. Cosmochim. Acta* **191**, 32–46.

Oelze M., Blanckenburg von F., Hoellen D., Dietzel M. and Bouchez J. (2014) Si stable isotope fractionation during adsorption and the competition between kinetic and equilibrium isotope fractionation: Implications for weathering systems. *Chem. Geol.* **380**, 161–171.

Opfergelt S. and Delmelle P. (2012) Silicon isotopes and continental weathering processes: Assessing controls on Si transfer to the ocean. *Comptes rendus - Geoscience* **344**, 723–738.

Opfergelt S., Burton K. W., Strandmann von P. A. E. P., Gislason S. R. and Halliday A. N. (2013) Riverine silicon isotope variations in glaciated basaltic terrains_ Implications for the Si delivery to the ocean over glacial–interglacial intervals. *Earth Planet. Sci. Lett* **369-370**, 211–219.

Opfergelt S., Cardinal D., André L., Delvigne C., Bremond L. and Delvaux B. (2010) Variations of δ30Si and Ge/Si with weathering and biogenic input in tropical basaltic ash soils under monoculture. *Geochim. Cosmochim. Acta* **74**, 225–240.

Opfergelt S., Cardinal D., Henriet C., Draye X., André L. and Delvaux B. (2006) Silicon Isotopic Fractionation by Banana (Musa spp.) Grown in a Continuous Nutrient Flow Device. *Plant Soil* **285**, 333–345.

Opfergelt S., Eiriksdottir E. S., Burton K. W., Einarsson A., Siebert C., Gislason S. R. and Halliday A. N. (2011) Quantifying the impact of freshwater diatom productivity on silicon isotopes and silicon fluxes: Lake Myvatn, Iceland. *Earth Planet. Sci. Lett* **305**, 73–82.

Pokrovsky O. S., Manasypov R. M., Loiko S., Shirokova L. S., Krickov I. A., Pokrovsky B. G., Kolesnichenko L. G., Kopysov S. G., Zemtzov V. A., Kulizhsky S. P., Vorobyev S. N. and Kirpotin S. N. (2015) Permafrost coverage, watershed area and season control of dissolved carbon and major elements in western Siberian rivers. *Biogeosciences* **12**, 6301–6320.

Pokrovsky O. S., Manasypov R. M., Loiko S. V., Krickov I. A., Kopysov S. G., Kolesnichenko L. G., Vorobyev S. N. and Kirpotin S. N. (2016) Trace element transport in western Siberian rivers across a permafrost gradient. *Biogeosciences* **13**, 1877–1900.

Pokrovsky O. S., Reynolds B. C., Prokushkin A. S., Schott J. and Viers J. (2013) Silicon isotope variations in Central Siberian rivers during basalt weathering in permafrost-dominated larch forests. *Chem. Geol.* **355**, 103–116.

Pokrovsky O. S., Schott J., Kudryavtzev D. I. and Dupré B. (2005) Basalt weathering in Central Siberia under permafrost conditions. *Geochim. Cosmochim. Acta* **69**, 5659–5680.

Pourpoint F., Templier J., Anquetil C., Vezin H., Trébosc J., Trivelli X., Chabaux F., Pokrovsky O. S., Prokushkin A. S., Amoureux J.-P., Lafon O. and Derenne S. (2017) Probing the aluminum complexation by Siberian riverine organic matter using solid-state DNP-NMR. *Chemical Geology* **452**, 1–8.

Reynolds B. C., Aggarwal J., André L., Baxter D., Beucher C., Brzezinski M. A., Engström E., Georg R. B., Land M., Leng M. J., Opfergelt S., Rodushkin I., Sloane H. J., van den Boorn S. H. J. M., Vroon P. Z. and Cardinal D. (2007) An inter-laboratory comparison of

Si isotope reference materials. *J. Anal. At. Spectrom.* **22**, 561–568.

Savage P. S., Georg R. B., Williams H. M., Burton K. W. and Halliday A. N. (2011) Silicon isotope fractionation during magmatic differentiation. *Geochim. Cosmochim. Acta* **75**, 6124–6139.

Sun X., Andersson P. S., Humborg C., Pastuszak M. and Mörth C.-M. (2013) Silicon isotope enrichment in diatoms during nutrient-limited blooms in a eutrophied river system. *J Geochem Explor.* **132**, 173–180.

Sun X., Olofsson M., Andersson P. S., Fry B., Legrand C., Humborg C. and Mörth C.-M. (2014) Effects of growth and dissolution on the fractionation of silicon isotopes by estuarine diatoms. *Geochim. Cosmochim. Acta* **130**, 156–166.

Sutton J. N., Varela D. E., Brzezinski M. A. and Beucher C. P. (2013) Species-dependent silicon isotope fractionation by marine diatoms. *Geochim. Cosmochim. Acta* **104**, 300–309.

Tréguer P. J. and De La Rocha C. L. (2013) The World Ocean Silica Cycle. *Annu. Rev. Marine. Sci.* **5**, 477–501.

Vorobyev S., Pokrovsky O., Serikova S., Manasypov R., Krickov I., Shirokova L., Lim A., Kolesnichenko L., Kirpotin S. and Karlsson J. (2017) Permafrost Boundary Shift in Western Siberia May Not Modify Dissolved Nutrient Concentrations in Rivers. *Water* **9**, 985–17.

Wetzel F., de Souza G. F. and Reynolds B. C. (2014) What controls silicon isotope fractionation during dissolution of diatom opal? *Geochim. Cosmochim. Acta* **131**, 128–137.

Ziegler K., Chadwick O. A., Brzezinski M. A. and Kelly E. F. (2005) Natural variations of δ30Si ratios during progressive basalt weathering, Hawaiian Islands. *Geochim. Cosmochim. Acta* **69**, 4597–4610.

**Figure captions**

Figure 1 Map of the Lena River watershed and sampling locations. Numbered black dots are sampling locations in the Lena, Viliui and Aldan Rivers, and red triangles are tributary sampling from the three following regions: Central Siberia Plateau (West), Verkhoyansk mountain range (East), Lena-Amganski Inter-River area (LAIRA, South). Blue star is the location of Yakutsk Station.

Figure 2 A. Rayleigh model fitted on the measured $\delta^{30}Si_{DSi}$ values in the Lena River main channel (long-dashed line) vs mixing line (dotted line) and the measured $\delta^{30}Si_{DSi}$ values of the Aldan and Viliui Rivers, *f* is fraction of remaining DSi; B. $\delta^{30}Si_{DSi}$ values vs. DSi in other tributaries in subareas of the Lena River watershed for the three regions mentioned on Figure 1.

Figure 3 $\delta^{30}Si_{DSi}$ in the tributaries from the Verkhoyansk mountain range. A. $\delta^{30}Si_{DSi}$ vs. DSi; B. $\delta^{30}Si_{DSi}$ vs. DSi/Na*+K (corrected for evaporite); C. $\delta^{30}Si_{DSi}$ vs. Al/Si; D. $\delta^{30}Si_{DSi}$ vs. temperature.

Figure 4 A. DSi concentrations (open symbols) and $\delta^{30}Si_{DSi}$ values (filled symbols with error bars) in the upstream of the Lena River (the Tabaga Hydrological Station) during summer-winter 2012-2013; B. the average DSi concentrations and $\delta^{30}Si_{DSi}$ values in the spring flood 2015.

Figure 5 A. $\delta^{30}Si_{DSi}$ vs 1/DSi of autumn-winter and spring flood samples; B. $\delta^{30}Si_{DSi}$ vs Al/Si in river water during spring flood

Table 1 Summary of temperature, pH, ions and Si isotope values of samples in July 2012 and June 2013. LR=the Lena River, AR=the Aldan River, VR=the Viliui River, CSP=Central Siberian Plateau, LAIRA=Lena-Amganski Inter-River Area, VMR=Verkhoyansk Mountain Range.

| Sample ID | Area | Sampling Date | Coordinates (Lat, Long) | T water[a] | pH[a] | Cond[a] (μS/cm[C]) | Alk (mM) | Na (mM) | K (μM) | Al (μM) | DSi (μM) | $\delta^{30}Si$ | $2\sigma_{sd}$ | $\delta^{29}Si$ | $2\sigma_{sd}$ |
|---|---|---|---|---|---|---|---|---|---|---|---|---|---|---|---|
| **Mainstream and major tributaries** | | | | | | | | | | | | | | | |
| LR2012-01 | LR | 2012-07-12 | 62.2626, 130.0172 | 16.7 | 6.8 | 90 | 0.9 | 0.28 | 15.9 | 4.4 | 78.7 | | | | |
| LR2012-02 | LR | 2012-07-12 | 63.3879, 129.5393 | 16.7 | 6.6 | 69 | 0.4 | 0.15 | 15.4 | 3.7 | 71.7 | | | | |
| LR2012-03 | LR | 2012-07-13 | 63.0194, 129.6847 | 17.2 | 6.5 | 84 | 0.6 | 0.24 | 15.3 | 4.4 | 78.0 | | | | |
| LR2012-04 | LR | 2012-07-14 | 62.1577, 129.9080 | 18.7 | 6.6 | 81 | 0.9 | 0.19 | 14.7 | 4.6 | 82.5 | 0.39 | 0.08 | 0.24 | 0.04 |
| LR2012-25 | LR | 2012-07-22 | 62.6492, 129.9074 | 19.6 | 6.9 | 90 | 3.6 | 0.19 | 13.9 | 2.9 | 83.3 | 0.41 | 0.08 | 0.31 | 0.04 |
| LR2012-28 | LR | 2012-07-24 | 61.2637, 128.7397 | 16.2 | 7.5 | 80 | 0.7 | 0.15 | 12.5 | 5.3 | 83.5 | | | | |
| LR2012-30 | LR | 2012-07-25 | 61.1079, 126.8905 | 16.9 | 7.7 | 125 | 1.9 | 0.37 | 14.3 | 3.2 | 75.9 | | | | |
| LR2012-31 | LR | 2012-07-26 | 60.8722, 125.6335 | 16.9 | 7.2 | 146 | 0.7 | 0.48 | 15.5 | 3.5 | 87.4 | 0.52 | 0.08 | 0.28 | 0.04 |
| LR2012-32 | LR | 2012-07-27 | 60.6092, 124.1885 | 15.7 | 7.9 | 174 | 0.8 | 0.39 | 15.6 | 3.1 | 78.1 | | | | |
| LR2012-34 | LR | 2012-07-27 | 60.8736, 125.6438 | 15.8 | 7.4 | 159 | 1.2 | 0.31 | 15.5 | 10.4 | 84.4 | | | | |
| LR2013-39 | LR | 2013-06-12 | 64.2183, 126.8644 | 12 | 7.6 | 101 | 2.9 | 0.04 | 12.7 | 2.5 | 58.7 | | | | |
| LR2013-41 | LR | 2013-06-13 | 64.3945, 126.3659 | 18.9 | 7.0 | 140 | 1.2 | 0.28 | 22.4 | 0.5 | 57.6 | 1.27 | 0.08 | 0.72 | 0.04 |
| LR2013-42 | LR | 2013-06-14 | 66.3439, 123.6759 | 15.1 | 7.3 | 139 | 1.9 | 0.36 | 22.8 | 1.5 | 62.3 | | | | |
| LR2013-45 | LR | 2013-06-15 | 68.7433, 123.9966 | 14.2 | 7.1 | 91 | 1.9 | 0.08 | 15.3 | 1.2 | 56.8 | 1.03 | 0.08 | 0.55 | 0.04 |
| LR2013-48 | LR | 2013-06-16 | 67.8737, 123.0923 | 16.1 | 7.1 | 121 | 4.0 | 0.34 | 21.6 | 1.3 | 59.6 | | | | |
| LR2013-49 | LR | 2013-06-16 | 67.9291, 123.0021 | 16.1 | 7.0 | 130 | 0.9 | 0.34 | 23.5 | 1.2 | 57.9 | | | | |
| LR2013-54 | LR | 2013-06-19 | 65.9486, 123.9140 | 19.5 | 7.1 | 128 | 1.1 | 0.31 | 22.3 | 0.9 | 55.4 | 0.90 | 0.08 | 0.46 | 0.06 |
| LR2013-57 | LR | 2013-06-21 | 65.0511, 124.8055 | 14.9 | 7.0 | 83 | 1.1 | 0.05 | 12.4 | 2.6 | 65.8 | 0.69 | 0.08 | 0.40 | 0.04 |
| LR2013-71 | LR | 2013-06-27 | 63.8859, 127.5421 | 16.1 | 7.4 | 85 | 1.0 | 0.05 | 11.8 | 2.1 | 68.9 | | | | |
| LR2013-73 | LR | 2013-06-27 | 63.4904, 128.8031 | 18.1 | 7.3 | 142 | 1.0 | 0.42 | 16.5 | 1.5 | 56.2 | | | | |
| LR2013-75 | LR | 2013-06-27 | 63.5282, 128.8600 | 16.3 | 7.6 | 92 | 0.5 | 0.06 | 12.1 | 2.1 | 69.0 | 0.46 | 0.10 | 0.31 | 0.09 |
| LR2013-78 | LR | 2013-06-28 | 63.1327, 129.6232 | 19.8 | 7.6 | 139 | 1.0 | 0.37 | 16.6 | 1.8 | 60.9 | 0.58 | 0.08 | 0.31 | 0.08 |
| LR2012-05 | AR | 2012-07-16 | 63.3495, 131.6771 | 18.3 | 7.1 | 91 | 0.6 | 0.05 | 11.3 | 4.0 | 76.4 | 0.57 | 0.08 | 0.30 | 0.04 |
| LR2012-08 | AR | 2012-07-17 | 63.2231, 133.2462 | 17.9 | 7.1 | 92 | 0.6 | 0.05 | 11.3 | 3.7 | 74.0 | | | | |
| LR2012-09 | AR | 2012-07-18 | 62.9229, 134.1728 | 18.4 | 7.5 | 94 | 0.6 | 0.05 | 11.9 | 3.8 | 82.9 | | | | |
| LR2012-11 | AR | 2012-07-18 | 62.7106, 134.6952 | 18.5 | 7.3 | 99 | 0.7 | 0.05 | 11.4 | 3.0 | 77.0 | 0.47 | 0.08 | 0.27 | 0.04 |
| LR2012-13 | AR | 2012-07-19 | 62.6383, 134.9219 | 19.1 | 7.7 | 86 | 0.8 | 0.06 | 11.3 | 3.2 | 80.9 | 0.48 | 0.08 | 0.26 | 0.04 |
| LR2012-22 | AR | 2012-07-21 | 63.4382, 129.6667 | 19.2 | 6.8 | 105 | 1.1 | 0.06 | 11.8 | 3.2 | 73.9 | | | | |
| LR2013-38 | AR | 2013-06-12 | 63.4339, 129.6398 | 10.9 | 7.4 | 86 | 0.8 | 0.04 | 12.3 | 2.3 | 61.7 | | | | |
| LR2013-40 | VR | 2013-06-13 | 64.3280, 126.3720 | 17.9 | 7.2 | 140 | 0.7 | 0.29 | 24.3 | 0.3 | 63.1 | | | | |
| LR2013-59 | VR | 2013-06-22 | 63.8700, 125.1667 | 20 | 7.2 | 110 | 0.7 | 0.23 | 18.7 | 0.5 | 66.2 | 1.37 | 0.08 | 0.68 | 0.04 |
| LR2013-60 | VR | 2013-06-23 | 63.9089, 123.1457 | 19.4 | 7.2 | 110 | 0.3 | 0.21 | 17.0 | 0.5 | 65.9 | 1.23 | 0.09 | 0.68 | 0.06 |
| LR2013-62 | VR | 2013-06-23 | 63.7582, 121.5983 | 20 | 7.4 | 111 | 0.9 | 0.25 | 18.4 | 0.6 | 70.1 | 1.38 | 0.08 | 0.72 | 0.08 |
| LR2013-66 | VR | 2013-06-24 | 64.0530, 126.3720 | 19.4 | 7.4 | 112 | 0.7 | 0.24 | 18.2 | 0.4 | 63.3 | | | | |
| **Other tributaries** | | | | | | | | | | | | | | | |
| LR2012-29 | CSP | 2012-07-25 | 61.1461, 126.8620 | 23.4 | 8.6 | 163 | 0.9 | 0.15 | 26.4 | 0.5 | 81.8 | 1.65 | 0.08 | 0.90 | 0.04 |
| LR2012-35 | CSP | 2012-07-28 | 61.1651, 126.9110 | 22.3 | 9.0 | 170 | 1.0 | 0.16 | 28.6 | 0.7 | 78.5 | | | | |
| LR2012-36 | CSP | 2012-07-28 | 61.1680, 126.8677 | 23.8 | 9.4 | 171 | 1.2 | 0.16 | 29.5 | 0.6 | 85.7 | | | | |
| LR2013-43 | CSP | 2013-06-14 | 66.7711, 123.3601 | 16.2 | 6.9 | 52 | 1.0 | 0.15 | 12.4 | 0.8 | 62.9 | 1.19 | 0.08 | 0.63 | 0.04 |
| LR2013-50 | CSP | 2013-06-16 | 67.8763, 123.0364 | 16.9 | 7.1 | 134 | 2.8 | 0.33 | 22.3 | 1.2 | 57.2 | 0.64 | 0.09 | 0.22 | 0.08 |
| LR2013-52 | CSP | 2013-06-17 | 67.2141, 123.1354 | 21.2 | 7.3 | 42 | 1.0 | 0.08 | 17.5 | 0.6 | 40.0 | 0.85 | 0.08 | 0.48 | 0.09 |
| LR2013-55 | CSP | 2013-06-21 | 64.9520, 124.5963 | 20.6 | 6.7 | 58 | 1.7 | 0.10 | 24.3 | 0.3 | 60.3 | 1.29 | 0.12 | 0.69 | 0.08 |
| LR2013-61 | CSP | 2013-06-23 | 63.7804, 121.5229 | 22.9 | 7.6 | 118 | 0.6 | 0.06 | 25.3 | 0.3 | 36.3 | 0.83 | 0.10 | 0.29 | 0.05 |
| LR2013-63 | CSP | 2013-06-24 | 64.0249, 123.8852 | 19.2 | 7.0 | 50 | 1.4 | 0.09 | 49.0 | 0.4 | 120.5 | 1.14 | 0.08 | 0.59 | 0.05 |
| LR2013-64 | CSP | 2013-06-24 | 64.0276, 124.0923 | 17.7 | 8.4 | 159 | 1.3 | 0.27 | 32.7 | 0.4 | 39.0 | | | | |
| LR2013-65 | CSP | 2013-06-24 | 64.0268, 124.3989 | 18.4 | 7.2 | 70 | 0.4 | 0.09 | 29.9 | 0.5 | 49.4 | | | | |
| LR2013-68 | CSP | 2013-06-26 | 64.1086, 126.7406 | 19.6 | 7.5 | 288 | 0.7 | 1.01 | 36.0 | 0.3 | 65.0 | | | | |
| LR2013-69 | CSP | 2013-06-26 | 63.9742, 127.0290 | 18.8 | 7.5 | 346 | 1.0 | 1.24 | 31.5 | 0.3 | 50.9 | 0.77 | 0.10 | 0.35 | 0.07 |
| LR2013-72 | CSP | 2013-06-27 | 63.4678, 128.7899 | 19.1 | 7.4 | 201 | 1.3 | 0.65 | 21.2 | 1.0 | 62.7 | 0.52 | 0.08 | 0.28 | 0.05 |
| LR2012-12 | LAIRA | 2012-07-19 | 62.6147, 134.9229 | 20.3 | 8.2 | 299 | 0.8 | 0.08 | 17.5 | 0.3 | 50.9 | 1.62 | 0.09 | 0.79 | 0.07 |
| LR2012-15 | LAIRA | 2012-07-19 | 62.9465, 134.0084 | 8.6 | 6.5 | 145 | 0.4 | 0.09 | 17.5 | 1.7 | 132.5 | | | | |
| LR2012-17 | LAIRA | 2012-07-20 | 63.0203, 133.4082 | 20.7 | 7.4 | 133 | 0.8 | 0.10 | 20.5 | 2.5 | 66.4 | 0.57 | 0.08 | 0.28 | 0.07 |
| LR2012-26 | LAIRA | 2012-07-24 | 61.9039, 129.8472 | 19 | 7.2 | 106 | 0.9 | 0.17 | 16.0 | 2.3 | 85.5 | 0.66 | 0.08 | 0.30 | 0.04 |
| LR2012-27 | LAIRA | 2012-07-24 | 61.2510, 128.7695 | 20.6 | 8.0 | 310 | 0.9 | 0.05 | 18.5 | 0.3 | 63.5 | | | | |
| LR2012-33 | LAIRA | 2012-07-27 | 60.5937, 124.2726 | 17.7 | 8.2 | 305 | 0.9 | 0.06 | 12.5 | 0.2 | 69.5 | 1.21 | 0.08 | 0.52 | 0.04 |
| LR2012-37 | LAIRA | 2012-07-29 | 61.1946, 128.2840 | 12.5 | 7.3 | 336 | 0.8 | 0.25 | 33.3 | 0.7 | 82.7 | 1.71 | 0.08 | 0.88 | 0.04 |
| LR2012-06 | VMR | 2012-07-16 | 63.3209, 131.9309 | 16.4 | 7.4 | 206 | 0.8 | 0.08 | 15.4 | 0.3 | 56.4 | | | | |
| LR2012-07 | VMR | 2012-07-17 | 63.2044, 133.2340 | 15.6 | 7.0 | 168 | 0.5 | 0.07 | 14.5 | 0.2 | 66.4 | 0.67 | 0.12 | 0.39 | 0.11 |
| LR2012-10 | VMR | 2012-07-18 | 62.7085, 134.7212 | 16.4 | 7.0 | 148 | 0.7 | 0.07 | 15.0 | 0.4 | 60.0 | 1.30 | 0.15 | 0.65 | 0.07 |
| LR2012-16 | VMR | 2012-07-20 | 63.1033, 134.0384 | 14.6 | 6.3 | 103 | 0.9 | 0.06 | 13.9 | 0.4 | 71.0 | 0.50 | 0.08 | 0.28 | 0.04 |
| LR2012-18 | VMR | 2012-07-20 | 63.3558, 131.7532 | 19.9 | 6.6 | 118 | 0.6 | 0.04 | 7.7 | 0.8 | 56.0 | | | | |
| LR2012-19 | VMR | 2012-07-20 | 63.3859, 133.1369 | 14.8 | 6.6 | 50 | 0.9 | 0.07 | 12.6 | 0.4 | 85.8 | | | | |
| LR2012-20 | VMR | 2012-07-20 | 63.3558, 131.7532 | 18 | 6.8 | 60 | 0.9 | 0.09 | 15.1 | 0.3 | 111.0 | | | | |
| LR2012-21 | VMR | 2012-07-21 | 63.3440, 130.3791 | 18.1 | 7.0 | 244 | 0.8 | 0.12 | 19.0 | 0.3 | 54.3 | 0.53 | 0.08 | 0.27 | 0.04 |
| LR2012-23 | VMR | 2012-07-21 | 63.4615, 129.5693 | 22.3 | 7.1 | 170 | 0.9 | 0.11 | 18.6 | 1.4 | 61.7 | 1.14 | 0.08 | 0.50 | 0.06 |
| LR2012-24 | VMR | 2012-07-21 | 63.5202, 129.3998 | 18.7 | 6.8 | 50 | 0.9 | 0.10 | 13.7 | 0.4 | 85.4 | 1.08 | 0.08 | 0.56 | 0.04 |
| LR2013-44 | VMR | 2013-06-15 | 68.7325, 124.0597 | 18.8 | 7.2 | 182 | 1.3 | 0.14 | 15.4 | 0.3 | 52.5 | 0.92 | 0.08 | 0.37 | 0.04 |
| LR2013-46 | VMR | 2013-06-15 | 68.3886, 123.9738 | 15.7 | 7.1 | 64 | 1.0 | 0.08 | 9.7 | 1.3 | 45.5 | 0.79 | 0.08 | 0.36 | 0.06 |
| LR2013-47 | VMR | 2013-06-16 | 68.0216, 123.4151 | 11.2 | 7.1 | 104 | 0.6 | 0.04 | 8.8 | 0.7 | 33.7 | | | | |
| LR2013-51 | VMR | 2013-06-17 | 67.2521, 123.4084 | 15.8 | 7.4 | 140 | 1.3 | 0.08 | 13.6 | 0.4 | 45.1 | 0.39 | 0.13 | 0.13 | 0.18 |
| LR2013-53 | VMR | 2013-06-18 | 66.2329, 124.1614 | 18.1 | 7.2 | 159 | 0.8 | 0.13 | 17.4 | 0.4 | 47.1 | 0.55 | 0.21 | 0.13 | 0.11 |
| LR2013-56 | VMR | 2013-06-21 | 65.0055, 124.9442 | 14.1 | 7.3 | 178 | 0.9 | 0.20 | 18.6 | 0.9 | 48.7 | 0.52 | 0.08 | 0.15 | 0.09 |
| LR2013-58 | VMR | 2013-06-22 | 64.6002, 125.7179 | 15.5 | 7.1 | 89 | 0.7 | 0.05 | 11.1 | 2.5 | 61.9 | 0.44 | 0.08 | 0.25 | 0.04 |
| LR2013-67 | VMR | 2013-06-26 | 64.1635, 126.9666 | 16.2 | 7.2 | 73 | 1.2 | 0.16 | 11.8 | 0.8 | 68.0 | | | | |
| LR2013-70 | VMR | 2013-06-26 | 64.0191, 127.3502 | 19.3 | 7.4 | 88 | 1.5 | 0.17 | 10.2 | 0.5 | 79.6 | 1.48 | 0.12 | 0.82 | 0.05 |
| LR2013-74 | VMR | 2013-06-27 | 63.5203, 128.8318 | 17 | 7.8 | 93 | 0.9 | 0.13 | 16.7 | 0.3 | 55.0 | 0.66 | 0.08 | 0.31 | 0.04 |
| LR2013-76 | VMR | 2013-06-28 | 63.5221, 129.3963 | 14.8 | 7.5 | 49 | 1.0 | 0.09 | 11.4 | 0.4 | 73.3 | | | | |
| LR2013-77 | VMR | 2013-06-28 | 63.4681, 129.5942 | 15.3 | 7.6 | 206 | 1.0 | 0.16 | 21.4 | 0.4 | 51.8 | | | | |

[a] is from Kutscher et al. 2017

Table 2 Water discharge, alkalinity, Al and Si concentrations with Si isotope values of winter and spring samples (water discharge 2012-2013 is the average monthly discharge; water discharge 2015 is daily discharge on the sampling day)

| Sampling time | Water discharge ($m^3/s$) | Alk (mM) | Al (μM) | DSi (μM) | $\delta^{30}Si$ | $2\sigma_{sd}$ | $\delta^{29}Si$ | $2\sigma_{sd}$ |
|---|---|---|---|---|---|---|---|---|
| **Autumn-winter samples taken monthly 2012-2013** | | | | | | | | |
| Sep 2012 | 34321 | 1.2 | N/A | 74.4 | 1.17 | 0.09 | 0.59 | 0.16 |
| Oct 2012 | 18259 | 1.2 | N/A | 98.3 | 1.57 | 0.09 | 0.91 | 0.06 |
| Nov 2012 | 4488 | 1.7 | N/A | 97.4 | 1.86 | 0.08 | 0.94 | 0.08 |
| Dec 2012 | 3641 | 2.1 | N/A | 126.8 | 1.66 | 0.22 | 0.9 | 0.04 |
| Jan 2013 | 4784 | 1.0 | N/A | 90.1 | 1.25 | 0.10 | 0.63 | 0.08 |
| Feb 2013 | 3398 | 3.0 | N/A | 171.7 | 1.65 | 0.09 | 0.85 | 0.07 |
| Mar 2013 | 2761 | 3.3 | N/A | 165.5 | 1.62 | 0.11 | 0.91 | 0.07 |
| **Spring flood samples taken daily in 2015** | | | | | | | | |
| May 06, 2015 | 107360 | 1.7 | 0.6 | 78.6 | 1.04 | 0.08 | 0.61 | 0.04 |
| May 08, 2015 | 141714 | 1.5 | 0.6 | 46.4 | 0.74 | 0.08 | 0.42 | 0.10 |
| May 11, 2015 | 149686 | 0.7 | 1.6 | 50.0 | 0.77 | 0.12 | 0.5 | 0.07 |
| May 14, 2015 | 100000 | 0.7 | 2.8 | 53.6 | 0.72 | 0.11 | 0.43 | 0.05 |
| May 17, 2015 | 78300 | 0.6 | 2.1 | 50.0 | 0.66 | 0.16 | 0.37 | 0.04 |
| May 20, 2015 | 69300 | 0.6 | 3.2 | 53.6 | 0.58 | 0.09 | 0.33 | 0.07 |
| May 23, 2015 | 62000 | 0.6 | 3.0 | 57.1 | 0.59 | 0.08 | 0.35 | 0.04 |
| May 26, 2015 | 60100 | 0.6 | 2.8 | 57.1 | 0.63 | 0.08 | 0.37 | 0.05 |
| May 28, 2015 | 61500 | 0.6 | 2.9 | 60.7 | 0.69 | 0.09 | 0.46 | 0.09 |

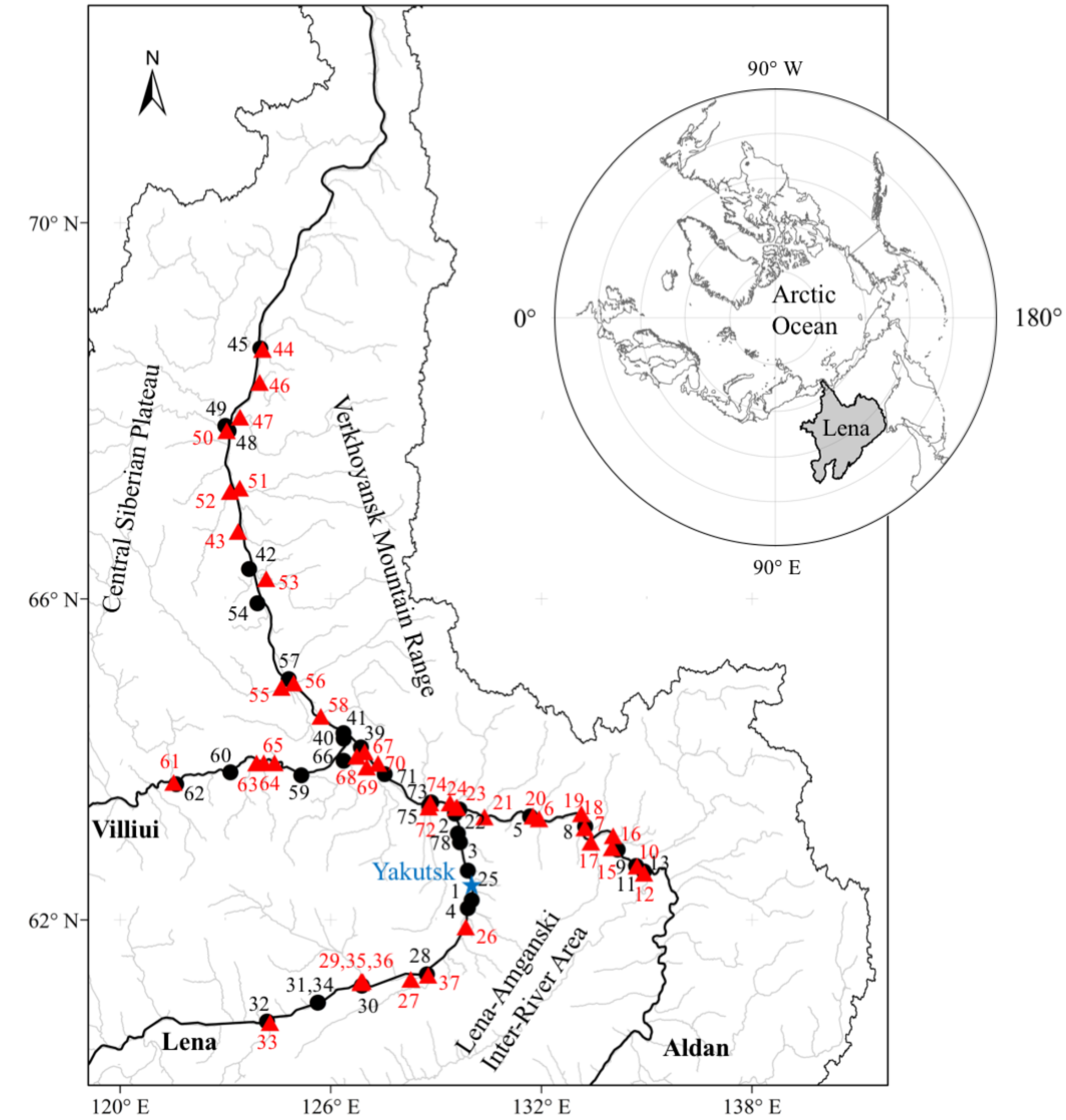
N
70° N
66° N
62° N
120° E
126° E
132° E
138° E
Central Siberian Plateau
Verkhoyansk Mountain Range
Lena-Amganski Inter-River Area
Villiui
Lena
Aldan
Yakutsk
90° W
90° E
0°
180°
Arctic Ocean
Lena

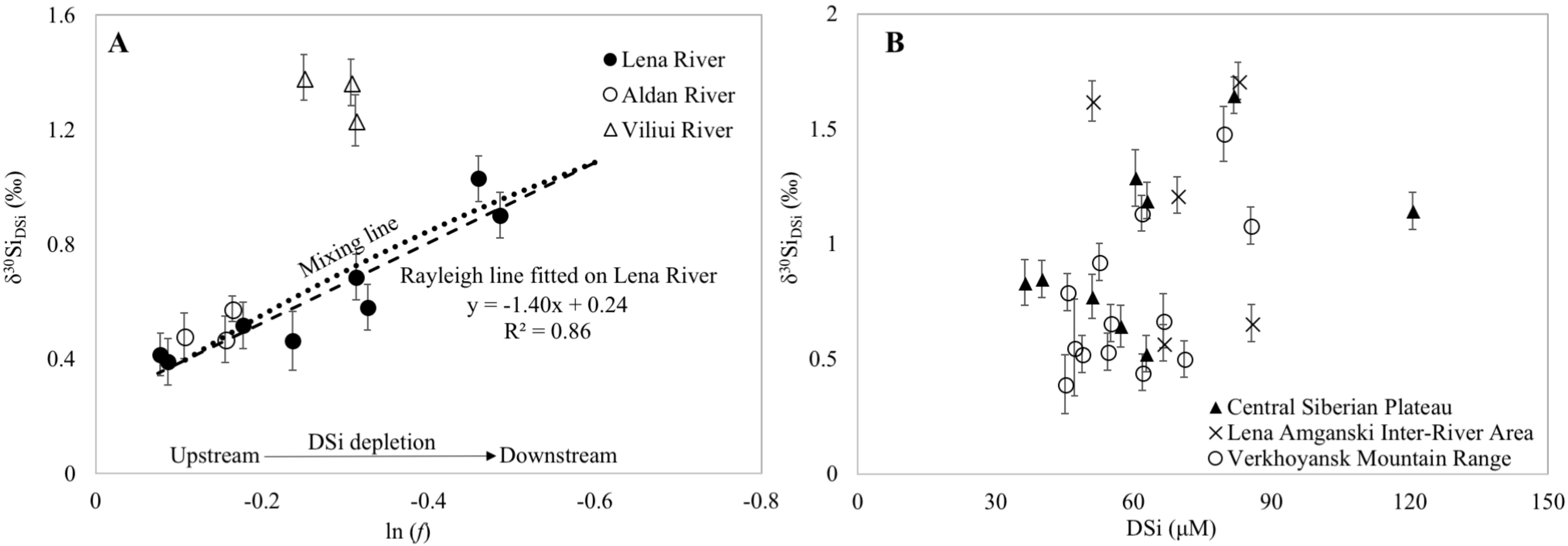
A
Lena River
Aldan River
Viliui River
Mixing line
Rayleigh line fitted on Lena River
y = -1.40x + 0.24
R² = 0.86
Upstream
DSi depletion
Downstream
δ30SiDSi (‰)
ln (f)
1.6
1.2
0.8
0.4
0
-0.2
-0.4
-0.6
-0.8
B
Central Siberian Plateau
Lena Amganski Inter-River Area
Verkhoyansk Mountain Range
DSi (μM)
2
1.5
1
0.5
30
60
90
120
150

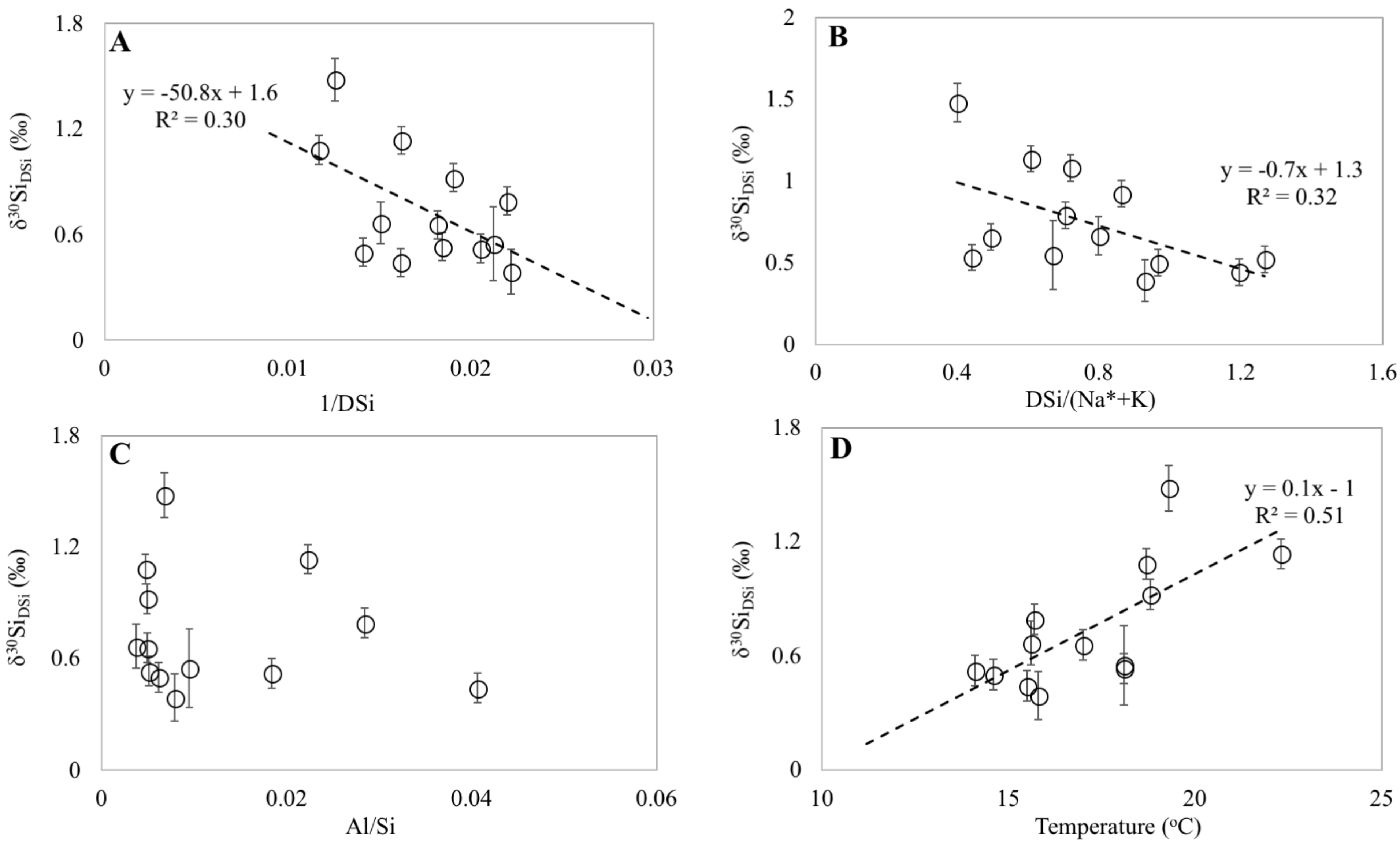
A
y = -50.8x + 1.6
R² = 0.30
δ30SiDSi (‰)
1/DSi
B
y = -0.7x + 1.3
R² = 0.32
δ30SiDSi (‰)
DSi/(Na*+K)
C
δ30SiDSi (‰)
Al/Si
D
y = 0.1x - 1
R² = 0.51
δ30SiDSi (‰)
Temperature (ºC)

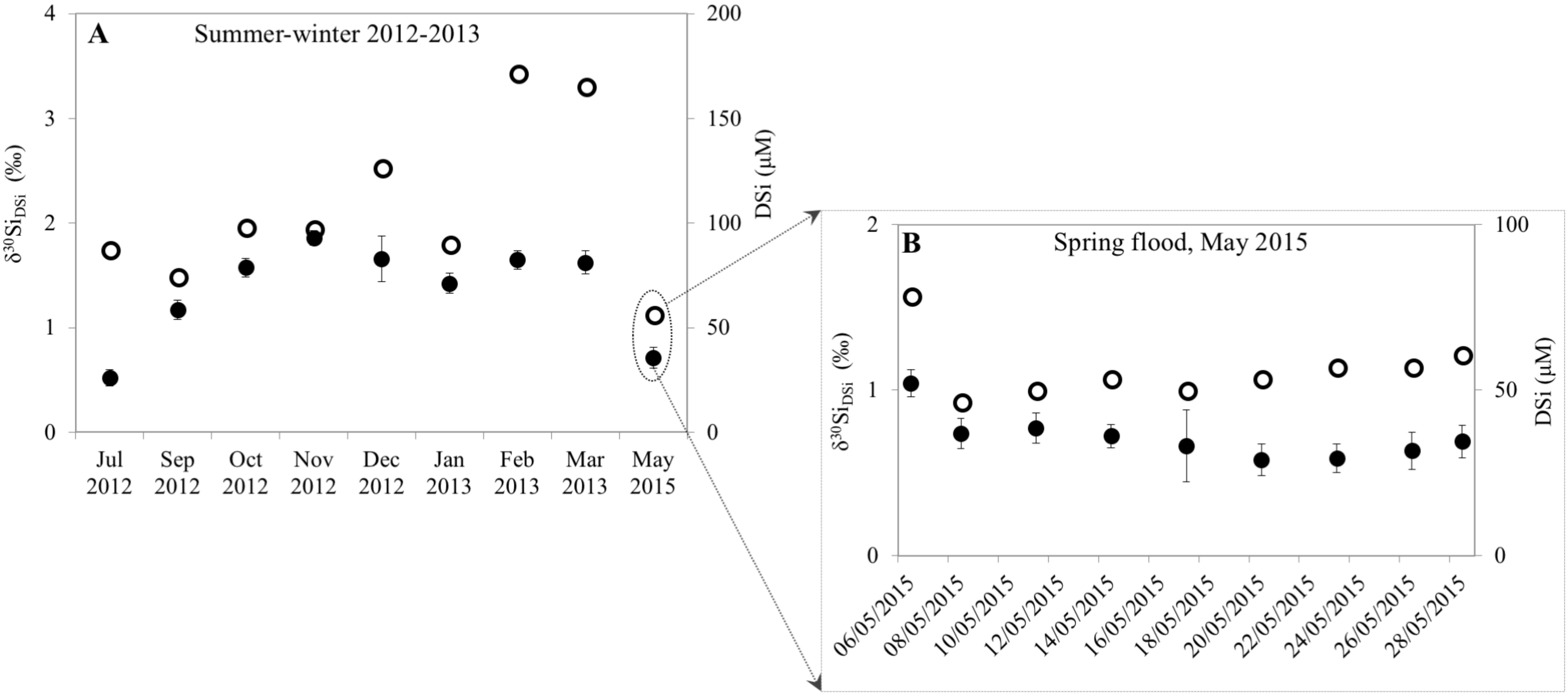
A
Summer-winter 2012-2013
δ30SiDSi (‰)
DSi (µM)
Jul 2012
Sep 2012
Oct 2012
Nov 2012
Dec 2012
Jan 2013
Feb 2013
Mar 2013
May 2015
B
Spring flood, May 2015
06/05/2015
08/05/2015
10/05/2015
12/05/2015
14/05/2015
16/05/2015
18/05/2015
20/05/2015
22/05/2015
24/05/2015
26/05/2015
28/05/2015

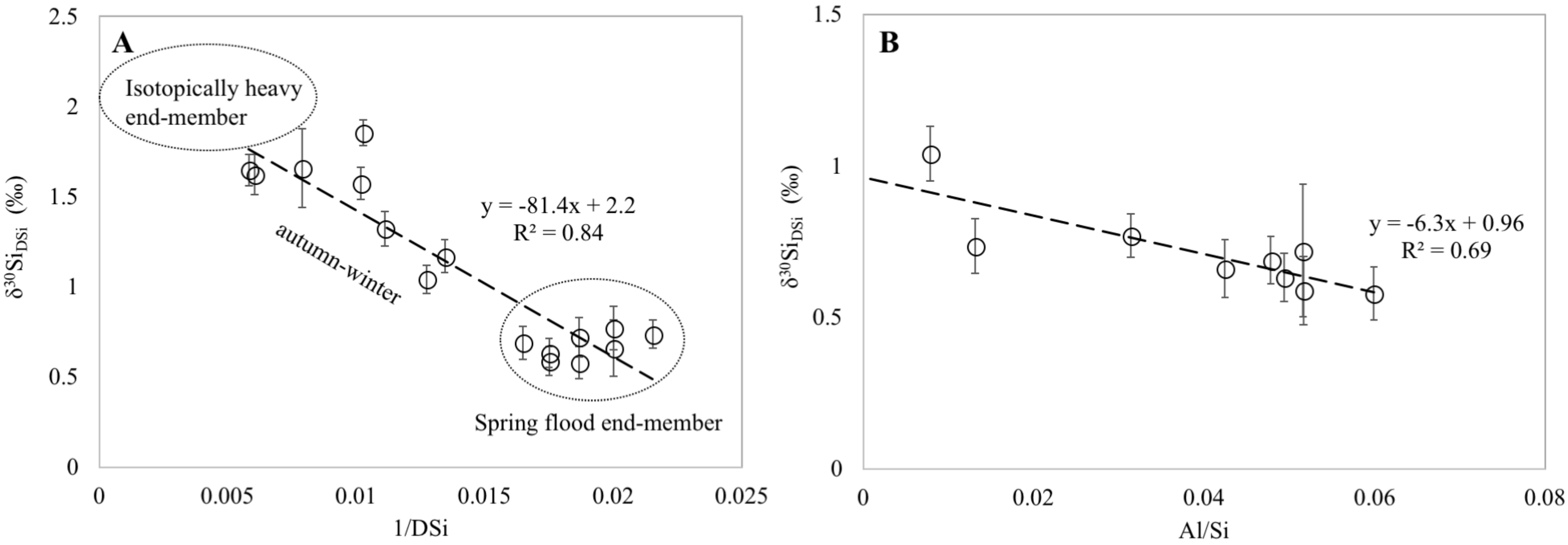

A
Isotopically heavy end-member
autumn-winter
y = -81.4x + 2.2
R² = 0.84
Spring flood end-member
δ30SiDSi (‰)
1/DSi
0
0.5
1
1.5
2
2.5
0.005
0.01
0.015
0.02
0.025
B
y = -6.3x + 0.96
R² = 0.69
δ30SiDSi (‰)
Al/Si
0.02
0.04
0.06
0.08

## Appendix

# Stable Silicon Isotopic Compositions of the Lena River and its Tributaries: Implications for Silicon Delivery to the Arctic Ocean

Xiaole Sun, Carl-Magnus Mörth, Don Porcelli, Liselott Kutscher, Catherine Hirst, Melissa Murphy, Trofim Maximov, Roman E. Petrov, Christoph Humborg, Melanie Schmitt, Per S. Andersson

Figure A1 Three Si isotope plot of Si standards and the samples in this study

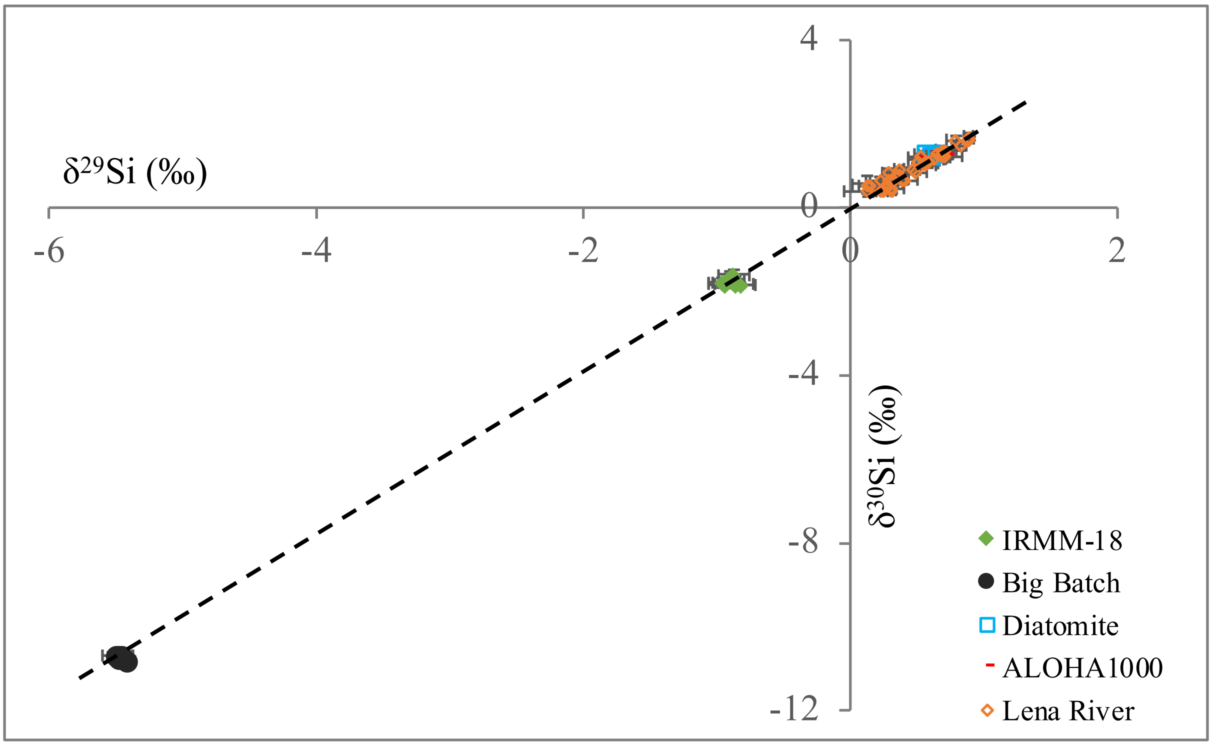


Table A1 The seasonal water discharge and DSi concentrations of the Lena River used for the Si flux-weighed annual $\delta^{30}Si_{DSi}$ value. The days of spring, summer and winter are counted as 61, 123 and 181 days, respectively (Data source: http://www.arcticgreatrivers.org/data.html).

| Water discharge of the Lena River ($m^3/s$) | | | |
|---|---|---|---|
| Year | Spring | Summer | Winter |
| 2010 | 37576 | 26588 | 3169 |
| 2011 | 35103 | 24143 | 4257 |
| 2012 | 47014 | 31322 | 3470 |
| 2013 | 47618 | 32902 | 3825 |
| 2014 | 51927 | 26438 | N/A |
| Average | 43847.6 | 28278.6 | 3680.3 |
| DSi concentrations of the Lena River (µM) | | | |
| Year | Spring | Summer | Winter |
| 2010 | 59.4 | 71.9 | 101.6 |
| 2011 | 52.1 | 81.3 | 103.1 |
| 2012 | 51.6 | N/A | 119.3 |
| 2013 | 42.2 | 164.1 | 241.7 |

# Appendix

| | | | |
|---|---|---|---|
| 2014 | 123.4 | 141.4 | N/A |
| Average | 65.7 | 114.6 | 141.4 |
| Total DSi flow (mol/season) | 15189.6 | 34454.4 | 8138.4 |
| Contribution percentage (%) | 26 | 60 | 14 |